Research Article

Combined effect of compressibility, height and thickness on the nonlinear behaviour of polyurethane, simply-supported spherical shells under apical loads

Bülent Yıldırım [1], Recep Faruk Yükseler [2]

[1] *Department of Civil Engineering, Pamukkale University, Kinikli, Denizli 20020, Turkey*
[2] *Department of Civil Engineering, Yildiz Technical University, Esenler, Istanbul 34220, Turkey*
* *Corresponding author: byildirim@pau.edu.tr*

Abstract

Previously, the effect of compressibility on the nonlinear buckling behaviour of thin, polyurethane, simply-supported spherical shells subjected to apical loads has been presented without considering the orders of the thickness and height of the spherical shells. In the meantime; it has been observed that although the variations of the thickness and height of the spherical shells do not affect the comments made for the effect of the compressibility on the buckling loads, they do affect the comments made for the effect of the compressibility on the buckling deflections considerably. In this study; combined effect of the compressibility, height and thickness on the buckling loads, buckling deflections and the apical load–apical deflection diagrams of polyurethane, thin, simply-supported spherical shells subjected to apical loads is investigated. Comparing the force–deflection diagrams corresponding to various values of the parameters pertaining to the compressibility of the material used, the height and the thickness of the shell; the variations of the buckling loads, buckling deflections and forms of the force–deflection diagrams corresponding to the various combinations of the mentioned parameters are discussed.

Keywords: Compressible material, finite difference method, nonlinear analysis, polyurethane, spherical shell

1. Introduction

Rubber-like materials, which are capable of making very large elastic deformations (Treolar 1975), have been dealt in various areas of science and technology. Although rubber-like materials have generally been assumed to be incompressible, the volume change due to deformation should be considered for some of the rubber-like materials (Blatz & Ko 1962; Simmonds 1987).

There have been many analytical, numerical and experimental studies on the behaviour of incompressible, rubber-like spherical shells under apical loads; considering only the geometrical nonlinearity (Parnell 1984; Ranjan & Steele 1977; Taber 1982), and considering both the geometrical and physical nonlinearities (Kocak & Yukseler 1999). On the other hand, the number of studies taking the compressibility of the materials into consideration (Simmonds 1987; Akyuz & Ertepinar 2001; Haddow & Faulkner 1974; Yukseler 1996a) has been small relative to those neglecting the compressibility on the behavior of the rubber-like shells.

Yıldırım & Yükseler (2011) have investigated the effect of the compressibility on the buckling behaviour of polyurethane spherical shells subjected to apical loads considering both the geometrical and physical nonlinearities. The present study is an extension of Yıldırım & Yükseler (2011) with the emphasis that investigating the effect of the compressibility on the force-deflection behaviour of rubber-like spherical shells under apical loads without considering the

magnitudes of height and thickness may be misleading. In section 2, the geometrical details of a shell element before and after deformation, constitutive equations of rubber-like shells and equations of equilibrium are given. The fundamental equations of a spherical shell, made of polyurethane, under an apical load are presented in Section 3. The application of finite differences and Newton-Raphson method to the governing equations of the problem are given in Section 4. In Section 5, numerical experiments pertaining to the behaviour of the apical force versus the apical deflection curves corresponding to the various combinations of the thickness, height of the spherical shell and the compressibility of the material used. Deductions corresponding to the numerical experiments are included in this section, as well. Concluding remarks are summarized in the last section, section 6.

Although the theoretical fundamentals of the present study coincide with those in Yıldırım & Yükseler (2011), the theoretical details given in Yıldırım & Yükseler (2011) have been presented again in this study in order for the completeness of the current presentation.

2. Geometry and governing equations

The geometry of a shell element is given in Figure 1. S is used to represent reference surface. φ is meridional angle and θ is parallel central angle. r and y are radial

coordinate and vertical coordinate on S, respectively. θ is parallel central angle. s_φ is meridional arc length. z is transverse coordinate.These definitions are used for the quantities belonging to the deformed shell.Hereafter, the subscript "0" is used to denote that the related parameter belongs to the undeformed configuration.
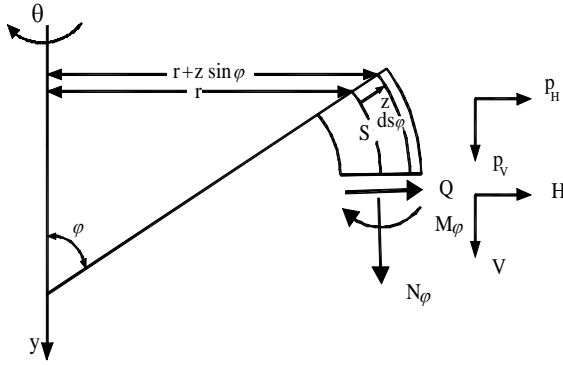
Figure 1. The geometry of a shell element .

2.1. Constitutive Relations

The constitutive equations can be written as:

$$N_\varphi = \frac{\partial w}{\partial \lambda_\varphi}, \quad N_\theta = \frac{\partial w}{\partial \lambda_\theta}, \quad M_\varphi = \frac{\partial w}{\partial K_\varphi}, \quad M_\theta = \frac{\partial w}{\partial K_\theta} \quad (1)$$

Taber (1987) where w is the two dimensional strain energy density function, M_φ and M_θ are bending moments, N_φ and N_θ are meridional stress resultant and normal stress resultant which is tangent to parallel circle, respectively; Q is transverse shear stress resultant (Figure 1); λ_φ and λ_θ are the stretchings at the directions of meridional and parallel circle tangent,respectively, which are on the reference surface ($z_0 = z = 0$); K_φ and K_θ are curvature change measures and

$$K_\varphi = k_\varphi - \lambda_\varphi^2 \lambda_\theta k_{\varphi_0} \quad (2)$$

$$K_\theta = k_\theta - \lambda_\theta^2 \lambda_\varphi k_{\theta_0} \quad (3)$$

where $k_{\varphi_0}, k_\varphi, k_{\theta_0}, k_\theta$ are curvature measures of undeformed and deformed reference surfaces (Yıldırım & Yükseler 2011). The constitutive equations (1) are valid for both the incompressible and compressible rubber-like shells of revolution.

2.2. Equations of Equilibrium

Force equilibrium and moment equilibrium equations Taber (1987) are

$$(r_0 V)' + r_0 p_V = 0 \quad , \quad (4)$$

$$(r_0 H)' - N_\theta + r_0 p_H = 0 \quad , \quad (5)$$

$$(r_0 M_\varphi)' - M_\theta \cos \varphi - r_0 (Q \lambda_\varphi) = 0 \quad , \quad (6)$$

means differentiation with respect to s_{φ_0} .Here; p_H and p_V are horizontal and vertical external forces acting per unit area of the reference surface of the undeformed shell, respectively, V is vertical stress resultant, H is horizontal stress resultant. N_φ and Q can be expressed in terms of H and V from the geometry as

$$N_\varphi = H \cos \varphi + V \sin \varphi \quad , \quad (7)$$

$$Q = H \sin \varphi - V \cos \varphi \quad . \quad (8)$$

3. Fundamental equations of a polyurethane spherical shell subjected to an apical load

The two dimensional strain energy function w of a polyurethane material is given as:

$$w = \frac{t\mu}{2}\left[\left[\lambda_\varphi^2 + \lambda_\theta^2 - p^{-1}\left(\lambda_\varphi \lambda_\theta\right)^{2p} - \frac{1+\upsilon}{\upsilon}\right] + \frac{t^2}{12(\lambda_\varphi \lambda_\theta)^{2(1+\upsilon)/(1-\upsilon)}}\left(\left[\frac{1+\upsilon}{1-\upsilon} + \lambda_\varphi^{2(1-\upsilon)}\lambda_\theta^{-2p}\right]\lambda_\theta^2 K_\varphi^2 \cdots\right.\right.$$

$$\left.\left. -4p\lambda_\varphi \lambda_\theta K_\varphi K_\theta + \left[\frac{1+\upsilon}{1-\upsilon} + \lambda_\varphi^{-2p}\lambda_\theta^{2/(1-\upsilon)}\right]\lambda_\varphi^2 K_\theta^2\right)\right] \quad (9)$$

where t is the thickness of the undeformed shell Simmonds (1987). μ and υ are material constants and υ is considered to be a measure of incompressibility and

$$p = \frac{\upsilon}{\upsilon - 1} . \quad (10)$$

For infinitesimally small strains, μ is equal to the shear modulus, and υ is equal to Poisson's ratio, and

$$\mu = E / 2(1+\psi), \quad \upsilon = \psi \quad (11)$$

where E and ψ are modulus of elasticity and Poisson's ratio, respectively. As υ approaches to 0.5, Eq. (9) has been noted to become the two dimensional strain energy density function of a neo-Hookean material, which is considered to be incompressible (Simmonds 1987). The governing equations related with a polyurethane spherical shell subjected to an apical loadcan be written as

$$h' = \lambda_\varphi \cos \varphi - \cos \varphi_0 \quad (12)$$

$$v' = \lambda_\varphi \sin\varphi - \sin\varphi_0 , \tag{13}$$

$$\chi' = K_\phi + \frac{1}{R_0}(\lambda_\phi^2 \lambda_\theta - 1) \tag{14}$$

$$H' = -\frac{\cos\varphi_0}{r_0}H + \frac{1}{r_0}\left[\mu t(\lambda_\theta - \lambda_\theta^{2p-1}\lambda_\varphi^{2p}) - \frac{\mu t^3 gB}{12\lambda_\phi^{2g}}\lambda_\theta^\gamma K_\phi^2 + \frac{\mu t^3}{12A}[-p\lambda_\theta^g \lambda_\varphi^{2u} K_\varphi^2 + B\lambda_\theta K_\varphi^2 \right.$$

$$\left. -2p\lambda_\varphi K_\theta K_\varphi + \frac{1}{u}\lambda_\theta^g \lambda_\varphi^{\frac{2}{u}} K_\theta^2]\right], \tag{15}$$

$$V' = -\frac{\cos\phi_0}{r_0}V \tag{16}$$

$$M_\varphi' = -\frac{\cos\varphi_0}{r_0}M_\varphi + \frac{\cos\varphi}{r_0}\left[\frac{\mu t^3}{12A}\left[-2p\lambda_\varphi \lambda_\theta K_\varphi + D\lambda_\varphi^2 K_\theta\right]\right] + H\lambda_\varphi \sin\varphi - V\lambda_\varphi \sin\varphi , \tag{17}$$

$$H\cos\varphi + V\sin\varphi = \mu t(\lambda_\varphi - \lambda_\varphi^{2p-1}\lambda_\theta^{2p}) - \frac{gB\mu t^3}{12}\lambda_\theta^{\frac{-4\upsilon}{1-\upsilon}}\lambda_\varphi^\Gamma K_\varphi^2$$

$$+ \frac{\mu t^3}{12A}[u\lambda_\varphi^{(1-2\upsilon)}\lambda_\theta^{\frac{2}{u}}K_\varphi^2 - 2p\lambda_\theta K_\varphi K_\theta - p\lambda_\theta^{\frac{2}{u}}\lambda_\varphi^g K_\theta^2 + D\lambda_\varphi K_\theta^2], \tag{18}$$

where R_0 is the radius of the undeformed shell, h is the radial displacement Yıldırım & Yükseler (2011),

$$h = r - r_0 , \tag{19}$$

v is the vertical displacement , i.e.

$$v = y - y_0 \tag{20}$$

χ is the rotation angle, and

$$\chi = \varphi - \varphi_0 \tag{21}$$

$$u = 1 - \upsilon \tag{22}$$

$$g = \frac{1+\upsilon}{u} \tag{23}$$

$$\gamma = \frac{-1-3\upsilon}{u} \tag{24}$$

$$A = \left(\lambda_\varphi \lambda_\theta\right)^{2g} , \tag{25}$$

$$B = g + \lambda_\varphi^{2u}\lambda_\theta^{-2p} , \tag{26}$$

$$D = g + \lambda_\varphi^{-2p}\lambda_\theta^{2/u} \tag{27}$$

$$p = \frac{-\upsilon}{1-\upsilon} = \frac{-\upsilon}{u} \tag{28}$$

$$\Gamma = \frac{-3-\upsilon}{1-\upsilon} \tag{29}$$

4. Numerical Approaches

Not being able to solve the problem analytically; the method of finite differences is applied to Eqs. (12-18), firstly, to convert them to algebraical equations and, then, the resulting algebraical difference equations are solved numerically by using the Newton Raphson method. A simply supported spherical shell with radius R_0 subjected to a concentrated apical load P, shown in Fig.2, is divided into *m* finite pieces, corresponding to *m+1* nodes, with the step length of Δs . φ_m is the meridianol angle at the support, and can be considered as a measure of the depth of the shell, as well.
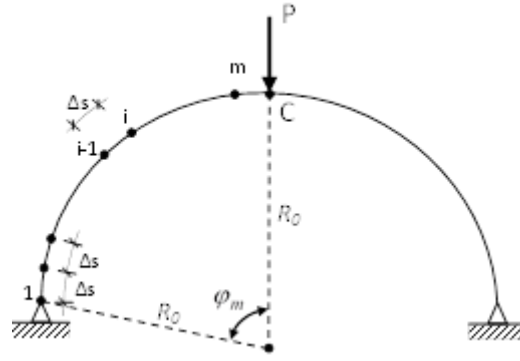
Figure 2. Discretization of the shell

The following algebraical equations are obtained if the finite difference equations are applied to Eqs. (12-18) for any point (*i*) (Yıldırım & Yükseler 2011):

$$h_{i+1} - h_i - \Delta s(\lambda_{\varphi_i} \cos \varphi_i - \cos \varphi_{0_i}) = 0 \quad , \tag{30}$$

$$v_{i+1} - v_i - \Delta s(\lambda_{\varphi_i} \sin \varphi_i - \sin \varphi_{0_i}) = 0 \quad , \tag{31}$$

$$\chi_{i+1} - \chi_i - \Delta s K_{\varphi_i} - \frac{\Delta s}{R_0}(\lambda_{\varphi_i}^2 \lambda_{\theta_i} - 1) = 0 \tag{32}$$

$$H_{i+1} - H_i + \frac{\Delta s \cos \varphi_0}{r_0} H_i - \frac{\Delta s}{r_0} N_\theta = 0 \tag{33}$$

$$V_{i+1} - V_i + \frac{\Delta s \cos \varphi_0}{r_0} V_i = 0 \quad , \tag{34}$$

$$M_{\varphi_{i+1}} - M_{\varphi_i} + \frac{\Delta s}{r_0} \cos \varphi_{0_i} M_{\varphi_i} - \frac{\Delta s}{r_0} \cos \varphi_i M_\theta - \Delta s H_i \lambda_{\varphi_i} \sin \varphi_i + \Delta s V_i \lambda_{\varphi_i} \cos \varphi_i = 0 \quad , \tag{35}$$

$$-H_i \cos \varphi_i - V_i \sin \varphi_i + \mu t(\lambda_{\varphi_i} - \lambda_{\varphi_i}^{2p-1} \lambda_{\theta_i}^{2p}) - \frac{gB\mu t^3}{12} \lambda_{\theta_i}^{-\frac{4\upsilon}{1-\upsilon}} \lambda_{\varphi_i}^\theta K_{\varphi_i}^2$$

$$+ \frac{\mu t^3}{12A}[u\lambda_{\varphi_i}^{(1-2\upsilon)} \lambda_{\theta_i}^{\frac{2u}{u}} K_{\varphi_i}^2 - 2p\lambda_{\theta_i} K_{\varphi_i} K_{\theta_i} - p\lambda_{\theta_i}^{\frac{2u}{u}} \lambda_{\varphi_i}^g K_{\theta_i}^2 + D\lambda_{\varphi_i} K_{\theta_i}^2] = 0 \tag{36}$$

At the points *i=1,2,...,m-1*, Eqs. (30-36) are used. At the point *m*; Eqs. (30-33) and Eqs. (35,36) are written using

$$h_C = \chi_C = 0 \tag{37}$$

where h_C and χ_C are the radial displacement and the rotation angle at the apex, respectively. λ_{φ_C} and V_C are removed from the unknown list. Instead of the concentrated apical load *P*, the apical vertical deflection v_C is given among the input data, in order to achieve the convergence of the iterations during the application of the Newton-Raphson method (Chapra & Canale 1994; Yıldırım 2007) in the vicinity of the region where the slope of the force-deflection curve is zero. The boundary equations for the point 1 are

$$h_1 = M_{\varphi_1} = v_1 = 0 \tag{38}$$

The total number of equations, *7m+2*, can be checked to be equal to the number of unknowns. The point load *P* at the apex can be obtained via

$$P = -V_1 . 2. \pi . r_{0_1} \tag{39}$$

which can be checked to be obtained through the equilibrium of the vertical forces for the whole shell.

5. Numerical Analysis

A Fortran program, which was prepared and mentioned in Yıldırım & Yükseler (2011), is used in the current study. A test of the accuracy of the proposed approach and the corresponding Fortran program have been dealt in Yıldırım & Yükseler (2011), comparing the numerical results of the prepared program with the experimental results of Taber (1982) in the problem of a hemispherical clamped shell under an apical load. Numerical experiments in order to understand the behavior of the apical force versus apical deflection curves and therefore the corresponding

buckling loads and buckling deflections of the simply supported polyurethane spherical shells, subjected to an apical load, with various thicknesses, depths and compressibilities are performed. A nondimensional thickness parameter, a nondimensional apical load, and nondimensional apical deflection, defined as:

$$\varepsilon = \frac{t}{R}, \; p^* = P/\mu t^2, \; v^* = v_C/R_0, \qquad (40)$$

are used, respectively. The force-deflection curves obtained in the numerical experiments for various values of the thickness parameter ε, the depth parameter φ_m and three different values of υ ($\upsilon = 0.0$, $\upsilon = 0.3$ and $\upsilon = 0.5$) are shown in Figures 3-11. $\upsilon = 0.5$ corresponds to incompressibility.
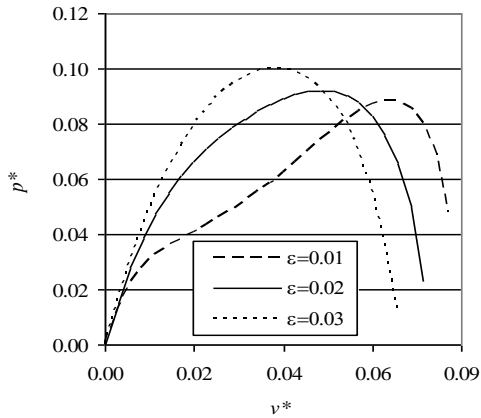
Figure 3. Force–deflection curves for $\varphi_m = \dfrac{\pi}{10}$, $\upsilon = 0.0$ and three different values of ε.

The curve corresponding to $\varepsilon = 0.02$ in this figure is named as form F1, for the comment made in the (*vi*)th deduction, given at the end of this section.
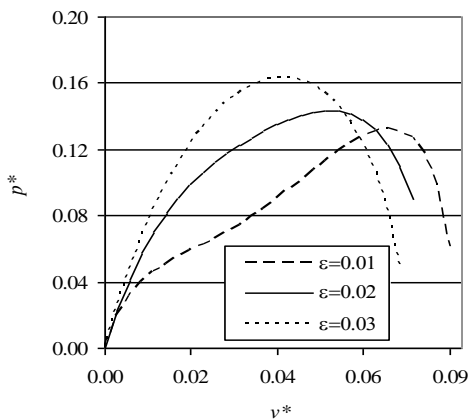
Figure 4. Force–deflection curves for $\varphi_m = \dfrac{\pi}{10}$, $\upsilon = 0.3$ and three different values of ε.
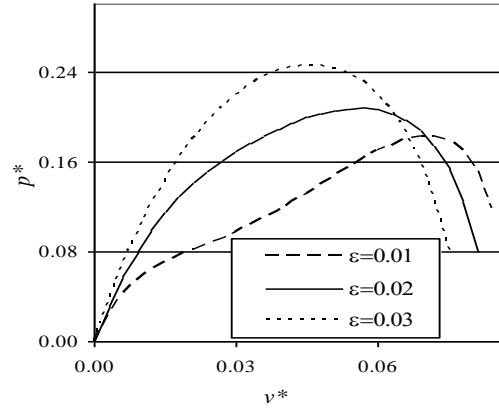
Figure 5. Force–deflection curves for $\varphi_m = \dfrac{\pi}{10}$, $\upsilon = 0.5$ and three different values of ε.
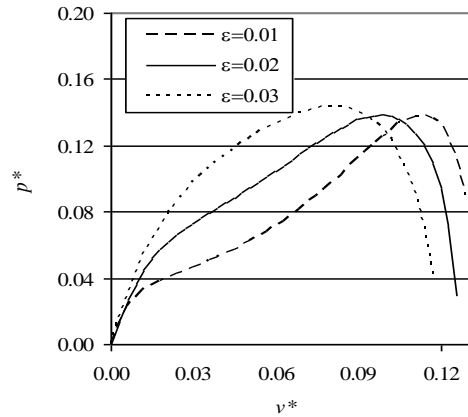
Figure 6. Force–deflection curves for $\varphi_m = \dfrac{\pi}{8}$, $\upsilon = 0.0$ and three different values of ε.
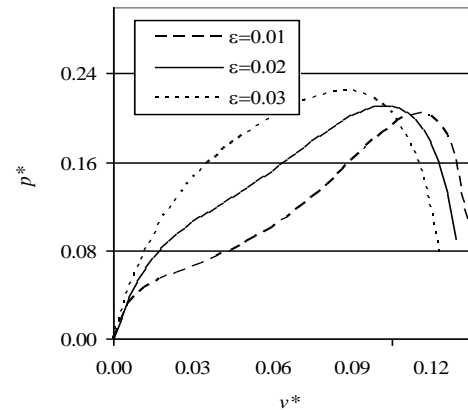
Figure 7. Force–deflection curves for $\varphi_m = \dfrac{\pi}{8}$, $\upsilon = 0.3$ and three different values of ε.
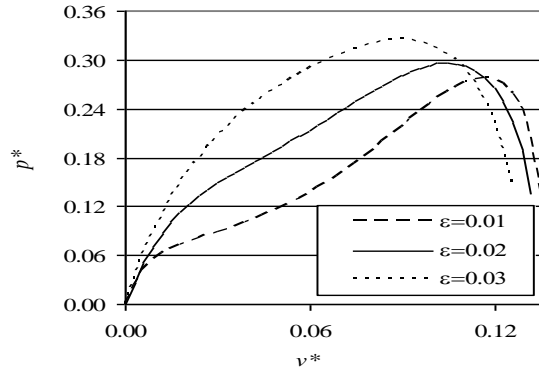
Figure 8. Force–deflection curves for $\varphi_m = \dfrac{\pi}{8}$, $\upsilon = 0.5$ and three different values of ε.
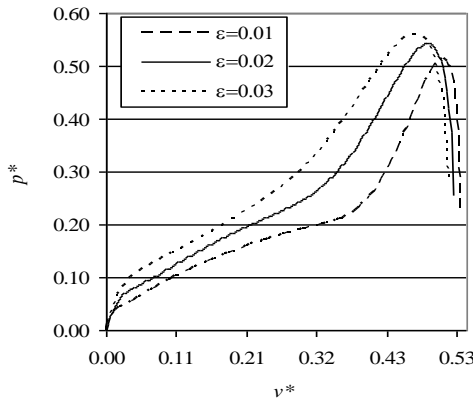
Figure 9. Force–deflection curves for $\varphi_m = \dfrac{\pi}{4}$, $\upsilon = 0.0$ and three different values of ε.
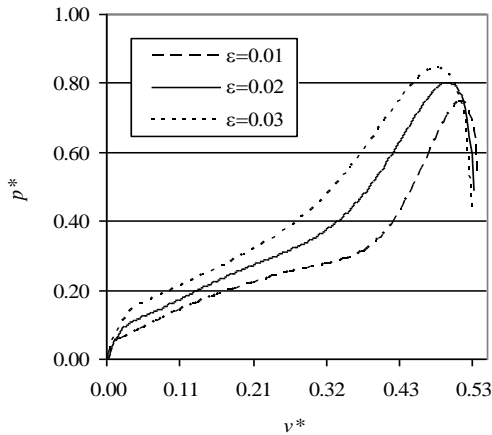
Figure 10. Force–deflection curves for $\varphi_m = \dfrac{\pi}{4}$, $\upsilon = 0.3$ and three different values of ε.

The curve corresponding to $\varepsilon = 0.02$ in this figure is named as form F2, for the comment made in the (*vi*)th deduction, given at the end of this section.
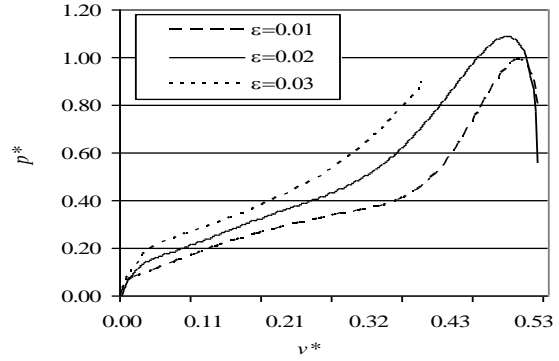
Figure 11. Force–deflection curves for $\varphi_m = \dfrac{\pi}{4}$, $\upsilon = 0.5$ and three different values of ε.

Knowing that the loads and deflections corresponding to the zero slope of the force-deflection curves (snap-through buckling, (Pfluger 1964), are the buckling loads p_{cr} and buckling deflections v_{cr}, respectively. The detailed numerical results of the nondimensional buckling loads and nondimensional buckling deflections corresponding to the various values of φ_m, ε and υ are tabulated in Table 1-2.

Table 1: Nondimensional buckling loads corresponding to various values of φ_m, ε and υ.

$\varphi_m = \dfrac{\pi}{10}$

ε \ υ	0.005	0.010	0.020	0.030	0.040	0.050
0.0	0.0866	0.0881	0.0921	0.1002	0.0998	0.0990
0.3	0.1266	0.1320	0.1434	0.1629	0.1701	0.1734
0.5	0.1706	0.1820	0.2074	0.2456	0.2644	0.2746

$\varphi_m = \dfrac{\pi}{8}$

ε \ υ	0.005	0.010	0.020	0.030	0.040	0.050
0.0	0.1307	0.1376	0.1383	0.1432	0.1530	0.1573
0.3	0.1902	0.2035	0.2113	0.2240	0.2457	0.2623
0.5	0.2550	0.2770	0.2962	0.3248	0.3679	0.4039

$\varphi_m = \dfrac{\pi}{4}$

ε \ υ	0.005	0.010	0.020	0.030	0.040	0.050
0.0	0.4995	0.5125	0.5427	0.5601	0.5680	0.5706
0.3	0.7110	0.7436	0.8038	0.8422	0.8658	0.8811
0.5	0.93253	0.9900	1.0879	-	-	-

From Figures 3-11 and Tables 1-2, the following statements can be deduced:

(i) As the values of φ_m (considered to be a measure of the height of the shell) are increased, the values of p_{cr} (buckling loads) and the values of v_{cr} (buckling deflections) are increased for all of the values of ε thickness parameter) and υ (measure of the compressibility), as in Yıldırım & Yükseler (2011).

Table 2: Nondimensional buckling deflections corresponding to various values of φ_m, ε and υ

$$\varphi_m = \frac{\pi}{10}$$

ε \ υ	0.005	0.010	0.020	0.030	0.040	0.050
0.0	0.0761	0.0669	0.0517	0.0395	0.0365	0.0395
0.3	0.0761	0.0699	0.0548	0.0456	0.0395	0.0426
0.5	0.0791	0.0699	0.0578	0.0456	0.0426	0.0456

$$\varphi_m = \frac{\pi}{8}$$

ε \ υ	0.005	0.010	0.020	0.030	0.040	0.050
0.0	0.1247	0.1156	0.1000	0.0821	0.0699	0.0639
0.3	0.1247	0.1186	0.1034	0.0882	0.0761	0.0669
0.5	0.1247	0.1186	0.1065	0.0913	0.0791	0.0699

$$\varphi_m = \frac{\pi}{4}$$

ε \ υ	0.005	0.010	0.020	0.030	0.040	0.050
0.0	0.5293	0.5110	0.4867	0.4684	0.4532	0.4380
0.3	0.5323	0.5141	0.4958	0.4806	0.4684	0.4563
0.5	0.5293	0.5141	0.4989	-	-	-

(ii) As the values of ε are increased, the values of p_{cr} are increased for all of the values of φ_m and υ, as in Yıldırım & Yükseler (2011).

(iii) As the values of υ are increased, the values of p_{cr} are increased for all of the values of ε and φ_m, as in Yıldırım & Yükseler (2011).

(iv) As the values of ε are increased, the values of v_{cr} are decreased for $\varphi_m = \frac{\pi}{4}$, $\varphi_m = \frac{\pi}{8}$ and all of the values of ε and υ; but, for $\varphi_m = \frac{\pi}{10}$ (the shallowest shell) and $\varepsilon = 0.05$ (the thickest shell, Novozhilov (1970), the values of v_{cr} are increased, unexpectedly, for all of the values of υ.

(v) As the values of υ are increased, the values of v_{cr} are increased for $\varphi_m = \frac{\pi}{8}$, $\varphi_m = \frac{\pi}{10}$ and all of the values of ε; but, for $\varphi_m = \frac{\pi}{4}$, the values of v_{cr} are passing through a maximum around $\upsilon = 0.3$ for all of the values of ε.

(vi) The forms of the force-deflection curves can be noted to be changing, as well as the concerning parameters are changed. If, typically, the form of the force-deflection curve corresponding to $\varepsilon = 0.02$, $\upsilon = 0.0$ and $\varphi_m = \frac{\pi}{10}$, shown in Figure 3, is named as $F1$ and the form of the force-deflection curve corresponding to $\varepsilon = 0.02$, $\upsilon = 0.3$ and $\varphi_m = \frac{\pi}{4}$, shown in Figure 10, is named as $F2$; the forms of the force-deflection curves can be noted to be changing from $F1$ to $F2$ as (a) φ_m is increased , (b) ε is decreased, and (c) υ is increased.

(vii) The phenomenon ofthesnap-through buckling has not been observed for $\varphi_m = \frac{\pi}{4}$, $\upsilon = 0.5$ and $\varepsilon \geq 0.03$, as seen in Tables 1-2.

6. Conclusions

It has been emphasized in this study that

(i) searching the effects of height, thickness and compressibility of the shells on the nonlinear buckling behaviour of compressible rubber-like shells one by one, without considering their various combinations, are misleading;

(ii) as the concerning parameters are changed, not only the values of the buckling loads and buckling deflections but also the forms of the force-deflection diagrams are changing.

References

Akyüz U, Ertepinar A (2001). Stability and breathing motions of pressurized compressible hyperelastic spherical shells. J Sound Vib 247, 293-304.

Blatz PJ, Ko WL (1962). Application of finite elastic theory to deformation of rubbery materials. Trans Soc Rhe 233-251.

Chapra SC, Canale RP (1994). Introduction to computing for engineers. Published by the McGraw-Hill, New York.

Haddow JB, Faulkner MG (1974). Finite expansion of a thick compressible spherical elastic shell. Int J Mech Sci 16, 63-73.

Koçak AE, Yükseler RF (1999). Finite axisymmetric strains and rotations of shellsof revolution with application to the problem of a spherical shell under a point load, 6th Annual International Conference on Composites Engineering, Florida, 421-422.

Novozhilov V (1970). Thin shells theory. Wolters-Noordhoff, Groningen.

Parnell TK (1984). Numerical improvement of asymtotic solutions and non-linear shell analysis. Stanford University, PhD Thesis.

Pflüger A (1964). Stabilitats probleme der elastostatic. Berlin.

Ranjan GV, Steele CR (1977). Large deflection of deep spherical shells under concentrated load, ASME/ASCE/AHS 18th Structures, Structurals Dynamics and Material Conference, 269-347.

Simmonds JG (1987). The strain- energy density of compressible, rubber-like axishells. ASME J App Mech 54, 453-454.

Taber LA (1982). Large deflection of a fluid-filled spherical shell under a point load. ASME J App Mech 49, 121-128.

Taber LA (1987). Large elastic deformation of shear deformable shells of revolution. ASME J App Mech 54, 578-584.

Treloar L.R.G. (1975). The Physics of Rrubber Elasticity. 3nd edition. Published by Clarendon Pres, Oxford.

Yıldırım B (2007). Nonlinear analysis of the simply supported spherical shells made of a compressible rubber-like material under the effect of an apical load. PhD thesis, YTU , Istanbul.

Yıldırım B, Yükseler RF (2011). Effect of compressibility on nonlinear buckling of simply supported polyurethane spherical shells subjected to an apical load. J Elast Plast 43, 167-187.

Yükseler RF (1996a). The strain energy density of compressible, rubber-like shells of revolution. ASME J App Mech 63, 419 – 423.